J Geod (2013) 87:813–823
DOI 10.1007/s00190-013-0648-x

ORIGINAL ARTICLE

# A technique for routinely updating the ITU-R database using radio occultation electron density profiles

**Claudio Brunini · Francisco Azpilicueta · Bruno Nava**

Received: 29 August 2012 / Accepted: 30 May 2013 / Published online: 13 June 2013


**Abstract** Well credited and widely used ionospheric models, such as the International Reference Ionosphere or NeQuick, describe the variation of the electron density with height by means of a piecewise profile tied to the F2-peak parameters: the electron density, $N_m$F2, and the height, $h_m$F2. Accurate values of these parameters are crucial for retrieving reliable electron density estimations from those models. When direct measurements of these parameters are not available, the models compute the parameters using the so-called ITU-R database, which was established in the early 1960s. This paper presents a technique aimed at routinely updating the ITU-R database using radio occultation electron density profiles derived from GPS measurements gathered from low Earth orbit satellites. Before being used, these radio occultation profiles are validated by fitting to them an electron density model. A re-weighted Least Squares algorithm is used for down-weighting unreliable measurements (occasionally, entire profiles) and to retrieve $N_m$F2 and $h_m$F2 values—together with their error estimates—from the profiles. These values are used to monthly update the database, which consists of two sets of ITU-R-like coefficients that could easily be implemented in the IRI or NeQuick models. The technique was tested with radio occultation electron density profiles that are delivered to the community by the COSMIC/FORMOSAT-3 mission team. Tests were performed for solstices and equinoxes seasons in high and low-solar activity conditions. The global mean error of the resulting maps—estimated by the Least Squares technique—is between $0.5\times10^{10}$ and $3.6\times10^{10}$ elec/m$^{-3}$ for the F2-peak electron density (which is equivalent to 7 % of the value of the estimated parameter) and from 2.0 to 5.6 km for the height (∼2 %).

**Keywords** Ionosphere · F2-peak parameters · ITU-R maps updating · International Reference Ionosphere (IRI) · NeQuick · Radio-occultation

C. Brunini · F. Azpilicueta (✉)
GESA, Facultad de Ciencias Astronómicas y Geofísicas, Universidad Nacional de La Plata, La Plata, Argentina
e-mail: azpi@fcaglp.unlp.edu.ar

C. Brunini
e-mail: claudio@fcaglp.unlp.edu.ar

C. Brunini · F. Azpilicueta
Consejo Nacional de Investigaciones Científicas y Técnicas, La Plata, Argentina

B. Nava
The Abdus Salam International Centre for Theoretical Physics, Trieste, Italy

## 1 Introduction

Well credited and widely used ionospheric models, such as the International Reference Ionosphere (IRI) (Bilitza 2001) or the NeQuick (Nava et al. 2008), describe the variation of the electron density with height by means of a piecewise profile tied to the F2-peak parameters: the electron density $N_m$F2, and the height $h_m$F2. Accurate values of these parameters are crucial for retrieving reliable electron density estimations from those models (Bilitza et al. 2012). The best option is to measure these parameters with an ionosonde or a incoherent scatter radar but, when this possibility is not available, IRI and NeQuick rely on the so-called ITU-R (Radio Communication Sector of the International Telecommunications Union) maps (ITU-R 1997). These maps are based on a pioneering work published in the early 1960s by William Jones and Roger Gallet (Jones and Gallet 1962, 1965; Jones and Obitts 1970), who developed an ad-hoc mapping technique (particularly well adapted to the computers

of their time) to compute monthly median values of the critical frequency $f_0$F2, and propagation factor $M_{3000}$F2, of the F2-peak (see Sect. 2.1). IRI or NeQuick models compute the values for the $N_m$F2 and $h_m$F2 driving parameters (see Sect. 2.2) using the ITU-R maps.

The ITU-R technique for computing the $f_0$F2 and $M_{3000}$F2 parameters depends on two sets of numerical coefficients (hereafter called the ITU-R database), one for low and the other for high solar activity. These coefficients were adjusted to data which were registered in the late 1950s on a network of ionosondes whose geographic distribution was rather inhomogeneous. For a solar activity level in between (outside) those defined for the database, the coefficients must be linearly interpolated (extrapolated). The ITU-R technique also requires the use of the 'modip' latitude (Rawer 1984), which depends on the geomagnetic inclination. Then to be consistent with the data used to build the maps, the geomagnetic field model of epoch 1960 should be used for computing the modip.

The present contribution is a work-in-progress report on a technique that we have developed to routinely update the ITU-R database using radio occultation electron density profiles (RO profiles) from the COSMIC/Formosat 3 mission (see Sect. 4.1). This development was guided by the interest in establishing a robust technique that could be automatically implemented in a computer and run autonomously and routinely to keep the database permanently updated. The technique takes advantage from the following facts: (i) the data used for updating the database are representative of the actual ionospheric conditions and related to the present geomagnetic field); (ii) at monthly intervals the data coverage is quite homogeneous both in space and in time; (iii) it avoids the linear interpolation/extrapolation between low and high solar activity periods, and (iv) at mid-latitudes the $N_m$F2 and $h_m$F2 values retrieved from RO profiles have proven to be in good agreement with ionosonde observations (Jakowski et al. 2004; Angling 2008). The main disadvantage is that RO profiles become less accurate at low latitudes. This effect is particularly evident in the equatorial anomaly region, where the electron density distribution presents strong spatial gradients (Schreiner et al. 2007; Yue et al. 201).

To mitigate the impact of this loss of accuracy, we have developed a special processing strategy consisting on fitting every single RO profile to our electron density model (i.e.: the La Plata Ionospheric Model, LPIM; see Sect. 2.2 and Brunini et al. 2011, 2013b), and carefully checking the statistical significance of the residuals obtained with the adjustment. This procedure eliminated a great amount of single electron density data marked as outliers and/or entire profiles that were considered as unreliable.

In Brunini et al. (2013b), we explored the possibility of using a spherical harmonic expansion with time-dependent coefficients—instead of the Jones and Gallet formalism—to directly map $h_m$F2—instead of $M_{3000}$F2. This way of modeling proved to accurately reproduce the $h_m$F2 values derived from the ITU-R maps, with the benefits of: (i) being better suited than the Jones and Gallet formalism for implementing a data assimilation scheme into the IRI or the NeQuick models; and (ii) avoid the intermediate step of transforming $M_{3000}$F2 into $h_m$F2. Based on that experience, for this work we decided to develop the technique to directly derive maps of $N_m$F2 and $h_m$F2 (instead of $f_0$F2 and $M_{3000}$F2) from the RO profiles.

The paper is organized as follows: Sect. 2 presents the background of this research, i.e.: the Jones and Gallet mapping technique, the relations that link $M_{3000}$F2 and $f_0$F2 to $h_m$F2 and $N_m$F2, and the ionospheric model used to assess the quality of the RO profiles. Section 3 describes the technique developed to obtain the updated databases for computing global maps of $h_m$F2 and $N_m$F2. This is done in a two-step procedure: (i) $h_m$F2 and $N_m$F2 values are retrieved from every RO profile and statically validated; (ii) the retrieved values are used to compute an ITU-R like database. Section 4 presents the dataset used in this research, the results obtained from these data after applying the technique previously developed and a short discussion about the differences between the $h_m$F2 and $N_m$F2 maps obtained with our technique and with the ITU-R database. The last section summarizes the research carried out and the conclusions extracted from the analysis.

Before closing this introduction, we would like to credit the efforts that have been made over the years to develop predictive models of the F2-peak parameters at global, regional or single site scale. These models are based on measurements provided by ground-based ionosondes in most cases, by incoherent scatter radars and space-based ionosondes in a fewer cases, and by GPS receivers onboard of low-orbiter satellites in the most recent studies. Among others, it is worth mentioning: Bilitza et al. (1979), Fox and McNamara (1988), Rush et al. (1989), Altinay et al. (1997), Wintoft and Cander (1999), Oyeyemi et al. (2005), Gulyaeva et al. (2008), Liu et al. (2008), Zhang et al. (2009), and Hoque and Jakowski (2011, 2012).

We also wish to point out that the development of the our technique has been guided by the intention of producing a database that can be used by the IRI and NeQuick models, without having to introduce significant changes in their source codes.

## 2 Background

### 2.1 The Jones and Gallet mapping technique

The mapping technique developed by Jones and Gallet (1962) provides values for $f_0$F2 and $M_{3000}$F2 anywhere in

the world at any time and for any given level of solar activity. Jones and Gallet preferred to map $M_{3000}$F2 instead of $h_m$F2 because its applicability in radio-propagation studies. $M_{3000}$F2 is defined by Eq. (1) where $f_0$F2 is the critical frequency of the F2 layer and maximum usable frequency (MUF) is the maximum frequency at which an electromagnetic signal emitted from the ground can reach another point on the ground 3000 km away from the transmitter.

$$M_{3000}\mathrm{F2} = \mathrm{MUF}/f_0\mathrm{F2}. \tag{1}$$

The sets $\{f_0\mathrm{F2},\ M_{3000}\mathrm{F2}\}$ and $\{N_m\mathrm{F2},\ h_m\mathrm{F2}\}$ are related through a system of equations that will be presented in the Sect. 2.2.

Jones and Gallet (1962) represented the daily variations of the parameters with Fourier series expansions as:

$$\Omega = a_0 + \sum_{j=1}^{J} [a_j \cdot \cos(j \cdot t) + b_j \cdot \sin(j \cdot t)], \tag{2}$$

where $\Omega$ is the parameter ($f_0$F2 or $M_{3000}$F2) to be mapped, $t$ is the Universal Time and $J$ is the maximum number of harmonics for mapping the diurnal variation: $J = 6$ for $f_0$F2 and $J = 4$ for $M_{3000}$F2. The spatial variation of these parameters is taken into account through the dependence of the Fourier coefficients on the geographic coordinates:

$$a_j = \sum_{k=0}^{K} U_{2j,k} \cdot G_k,\ \ j \geq 0 \quad \text{and}$$
$$b_j = \sum_{k=0}^{K} U_{2j-1,k} \cdot G_k,\ \ j \geq 1, \tag{3}$$

where $K = 75$ for $f_0$F2 and $K = 49$ for $M_{3000}$F2, $U_{1,0}, \ldots, U_{2J,K}$ are the numerical coefficients of the expansion (988 for $f_0$F2 and 441 for $M_{3000}$F2), and $G_0, \ldots, G_K$ are special functions whose explicit form depends on the $k$ index, for example

$$G_{54} = \sin^8(\mu) \cdot \cos^2(\varphi) \cdot \cos(2 \cdot \lambda), \tag{4}$$

where $\phi$ and $\lambda$ are the geographic latitude and longitude and $\mu$ is the so-called modip latitude (Rawer 1984), defined by:

$$\mu = arc\tan\left(\frac{I}{\sqrt{\cos(\varphi)}}\right), \tag{5}$$

where $I$ is the magnetic inclination at an altitude of 350 km above the Earth's surface.

The numerical coefficients $U_{1,0}, \ldots, U_{2J,K}$ of Eq. (3) were estimated by means of a Least Squares adjustment to a set of observations collected from 1954 to 1958 at a network of around 150 ionosondes with an uneven global distribution. This procedure led to establish two sets of coefficients for each parameter to be mapped for every month of the year (one set for low and the other for high solar activity). The solar activity level enters into the model with the so-called $R_{12}$ parameter which is the 12-month running mean value of the monthly mean sunspot number. For a given month and a $R_{12}$ value between $R_{12} = 0$ (low) and $R_{12} = 100$ (high solar activity), the coefficients are linearly interpolated from the tabulated values. For $R_{12} > 100$ the coefficients are extrapolated.

### 2.2 The relation between ($f_0$F2, $M_{3000}$F2) and ($N_m$F2, $h_m$F2)

$N_m$F2 and $f_0$F2 parameters are related through a simple relation (Bilitza 2002):

$$N_m\mathrm{F2} = 1.24 \times 10^{10} \cdot f_0\mathrm{F2}^2, \tag{6}$$

where $f_0$F2 is measured in MHz and $N_m$F2 in elec/m$^{-3}$.

The relation between $h_m$F2 and $M_{3000}$F2 has been an active subject of study. Shimazaki (1955) proposed an empirical relationship (based on the strong anti-correlation observed between the mentioned parameters) with the form:

$$h_m\mathrm{F2} = \frac{1490}{M_{3000}\mathrm{F2}} - 176, \tag{7}$$

where $h_m$F2 is in km. This equation evolved to a more complex one after the works of Wright and Mcduffie (1960), Bradley and Dudeney (1973), Eyfrig (1973), Dudeney (1975), Bilitza et al. (1979), Obrou et al. (2003), and Rawer and Eyfrig (2004). In this paper we used the equation established by Bilitza et al. (1979):

$$h_m\mathrm{F2} = \frac{1490}{M_{3000}\mathrm{F2} + \mathrm{CF}} - 176, \tag{8}$$

with the correction factor given by:

$$\mathrm{CF} = \frac{[0.00232 \cdot R + 0.222] \cdot \left[1 - \frac{R}{150}\exp(-\frac{\vartheta^2}{1600})\right]}{\frac{f_0\mathrm{F2}}{f_0E} - 1.2 - 0.0116 \cdot \exp(0.0239 \cdot R)} + 0.096 \cdot \frac{(R - 25)}{150}, \tag{9}$$

$R$ being the sunspot number, $\vartheta$ the geomagnetic latitude and $f_0E$ the critical frequency of the ionospheric E layer.

### 2.3 The LPIM electron density vertical profile

The model used to represent the electron density vertical profile used in this work is the one implemented in the La Plata Ionospheric Model (LPIM) (Brunini et al. 2013a). It uses three $\alpha$-Chapman layers (corresponding to the three characteristic ionospheric layers) to compute the electron density $N$ as a function of the height $h$:

$$N_i(h) = N_{mi} \cdot \exp\frac{1}{2} \cdot \left[1 - \frac{h - h_{mi}}{H_i} - \exp\left(-\frac{h - h_{mi}}{H_i}\right)\right], \tag{10}$$

where the sub-index $i = 1, 2, 3$, identifies the layers E, F1 and the bottom-side of the F2, and $N_{mi}$, $h_{mi}$ and $H_i$ are the maximum electron density, the height of that maximum, and the scale height of the corresponding layer (i.e., $N_{m3} \equiv N_m\mathrm{F2}$, $h_{m3} \equiv h_m\mathrm{F2}$, and $H_3 \equiv H\mathrm{F2}$).

The electron density in the top-side is represented with a vary-Chapman function (Reinisch and Huang 2001):

$$N_4(h) = N_{m3} \cdot \sqrt{\frac{H_3}{H_4(h)}} \cdot \exp\frac{1}{2} \times \left[1 - \int_{h_{m,3}}^{h} \frac{d\zeta}{H_4(\zeta)} - \exp\left(-\int_{h_{m,3}}^{h} \frac{d\zeta}{H_4(\zeta)}\right)\right], \quad (11)$$

with $\zeta$ going from the lower to the upper integration limit. $H_4(h)$ is the height-varying scale height given by:

$$H_4(h) = H_T + \frac{H_3 - H_T}{\tanh(p)} \cdot \tanh\left(p \cdot \frac{h - h_T}{h_{m3} - h_T}\right). \quad (12)$$

where $h_T$ is the transition height where the dominant ion specie changes from $O^+$ to $H^+$, $H_T$ is the scale height at the transition height and $p$ is the shape parameter of the topside profile. All of them are evaluated according to Meza et al. (2008).

In summary, the electron density computed with the LPIM profile at any given height can be expressed as:

$$N(h) = \begin{cases} \sum_{i=1}^{3} N_i(h), & \text{if } h \le h_{m3} \\ N_4(h), & \text{if } h > h_{m3} \end{cases}. \quad (13)$$

with $N_i(h)$ given by Eq.(10).

The shape of the LPIM profile is determined by the F2 peak parameters ($N_{m3} \equiv N_m\mathrm{F2}$, $h_{m3} \equiv h_m\mathrm{F2}$, $H_3 \equiv H\mathrm{F2}$) because once they are fixed, LPIM computes all the other parameters according to the ITU-R recommendations:

$$\left.\begin{array}{l} N_{m1} = A_1 \cdot \cos^{n_1}\chi \\ h_{m1} = 120km \\ H_1 = 5.0 + h_{m3} - h_{m1} \end{array}\right\} \text{E layer}, \quad (14)$$

$$\left.\begin{array}{l} N_{m2} = A_2 \cdot \cos^{n_2}\chi \\ h_{m2} = 165 + 0.6 \cdot \chi \\ H_2 = 0.4 \cdot (h_{m3} - h_{m1}) \end{array}\right\} \text{F1 layer}, \quad (15)$$

where $\chi$ is the solar zenith angle, $A_1$, $A_2$, $n_1$ and $n_2$ are functions that depend on the geographic latitude and the solar activity level. The explicit forms of them are contained in the ITU-R (1997) recommendations.

For a given location (latitude, longitude and height) and time, the LPIM electron density prediction is given by a function that depends on the three parameters, $N_m\mathrm{F2}$, $h_m\mathrm{F2}$ and $H\mathrm{F2}$; symbolically:

$$N(\phi, \lambda, h, t; N_m\mathrm{F2}, h_m\mathrm{F2}, H\mathrm{F2}). \quad (16)$$

In Brunini et al. (2013a) we described the LPIM model together with a data assimilation technique that is the basis for the data analysis procedure described in the next section. In that paper we also assessed the model performances by comparing its predictions to a dataset independent of the one assimilated into the model. After assimilating ground-based GNSS measurements and RO profiles we compared the LPIM-derived vertical total electron content (vTEC) estimation to Jason1 (J1) mission determinations. The comparison was performed for a complete year of low solar activity and showed a quite good agreement between model and measurements. 99 percent of the differences—LPIM minus J1 vTEC—did not exceed the range of $[-0.5, -3.4]$ total electron content units (TECu). The mean difference showed a systematic bias of $-1.3$ TECu (LPIM lower than Jason 1 vTEC), which is in accordance to the results reported by other authors (e.g., Codrescu et al. 2001; Hernandez-Pajares 2003; Delay and Doherty 2004; Brunini et al. 2005; Azpilicueta and Brunini 2008).

## 3 The technique for updating the ITU-R database

### 3.1 Retrieving $N_m\mathrm{F2}$ and $h_m\mathrm{F2}$ from RO electron density vertical profiles

The process of estimating the $N_m\mathrm{F2}$ and $h_m\mathrm{F2}$ parameters from the RO profiles consisted on adjusting (by Least Squares) the LPIM profile to every RO profile available for the time period of interest. For doing this, we used the linearized form of Eq. (16) to obtain the following equation of observation:

$$N_{\mathrm{obs}} = N_{\mathrm{pri}} + \frac{\partial N}{\partial N_m\mathrm{F2}} \cdot \Delta N_m\mathrm{F2} + \frac{\partial N}{\partial h_m\mathrm{F2}} \cdot \Delta h_m\mathrm{F2} + \frac{\partial N}{\partial H\mathrm{F2}} \cdot \Delta H\mathrm{F2} + v, \quad (17)$$

where $N_{\mathrm{obs}}$ is the electron density value from the RO profile; $N_{\mathrm{pri}}$ is the corresponding electron density value computed with a priori values $N_m\mathrm{F2}_{\mathrm{pri}}$, $h_m\mathrm{F2}_{\mathrm{pri}}$ and $H\mathrm{F2}_{\mathrm{pri}}$; $\frac{\partial N}{\partial N_m\mathrm{F2}}$, $\frac{\partial N}{\partial h_m\mathrm{F2}}$ and $\frac{\partial N}{\partial H\mathrm{F2}}$ are the LPIM derivatives with respect to the F2 peak parameters; $\Delta N_m\mathrm{F2} = N_m\mathrm{F2}_{pos} - N_m\mathrm{F2}_{\mathrm{pri}}$, $\Delta h_m\mathrm{F2} = h_m\mathrm{F2}_{pos} - h_m\mathrm{F2}_{\mathrm{pri}}$ and $\Delta H\mathrm{F2} = H\mathrm{F2}_{pos} - H\mathrm{F2}_{\mathrm{pri}}$, are the correction to the a priori that would be estimated with the Least Squares adjustment; and $v$ is the deviation between the measured and a posteriori computed electron density value.

The a priori values for $N_m\mathrm{F2}$ and $h_m\mathrm{F2}$ (i.e.: $N_m\mathrm{F2}$ and $h_m\mathrm{F2}_{\mathrm{pri}}$) were computed using the Jones and Gallet (1962) mapping technique to obtain $f_0\mathrm{F2}_{\mathrm{pri}}$ and $M_{3000}\mathrm{F2}_{\mathrm{pri}}$, and then, the Eqs. (6), (8) and (9) to convert $f_0\mathrm{F2}_{\mathrm{pri}}$ and $M_{3000}\mathrm{F2}_{\mathrm{pri}}$ into $N_m\mathrm{F2}_{\mathrm{pri}}$ and $h_m\mathrm{F2}_{\mathrm{pri}}$. The a priori value for $H\mathrm{F2}$ (i.e.: $H\mathrm{F2}_{\mathrm{pri}}$) was computed from $f_0\mathrm{F2}_{\mathrm{pri}}$ and $M_{3000}\mathrm{F2}_{\mathrm{pri}}$, using the empirical relation adopted by LPIM

(Brunini et al. 2013a), which are in accordance with the ITU-R (1997) recommendations:

$$HF2_{pri} = \frac{4.774 \cdot f_0F2_{pri}^2}{\exp(-3.467 + 1.714 \cdot \log(f_0F2_{pri}) + 2.02 \cdot \log(M_{3000}F2_{pri}))} \quad (18)$$

where $f_0$F2 is measured in MHz and $H$F2in km.

The corrections $\Delta N_m$F2, $\Delta h_m$F2 and $\Delta H$F2 were estimated along with their standard deviations by means of a re-weighted Least Squares procedure. All the weights were initially set to the same value and then were iteratively modified according to the difference between the RO electron density determination and value predicted by the model with previous solution. The weighting criterion was the 'bisquare' function described by Huber (1981). The iteration was stopped when the changes in the solution became negligible.

### 3.2 Building the database

To overcome the computational limitations of their time, Jones and Gallet (1962) constructed the special basis of mathematical functions like the one presented in Eq. (4). This basis fulfilled the condition of orthogonality with respect to the geographic configuration of the data sample, which avoided the inversion of the normal matrix. Based on the encouraging results obtained in (Brunini et al. 2013b), we changed the Jones and Gallet's formulation by a spherical harmonic expansion series with time-dependent coefficients, and directly mapped the $N_m$F2 and $h_m$F2 instead of $f_0$F2 and $M_{3000}$F2 parameters (primary parameters of the IRI and NeQuick models). This way of modeling implies that Eqs. (3) shall be replaced by:

$$\begin{cases} a_j = \sum_{l=0}^{L} \sum_{m=0}^{l} \left[ A^c_{jlm} \cdot \cos(m \cdot \lambda) + A^s_{jlm} \cdot \sin(m \cdot \lambda) \right] \cdot P_{lm}(\sin \mu) \\ b_j = \sum_{l=0}^{L} \sum_{m=0}^{l} \left[ B^c_{jlm} \cdot \cos(m \cdot \lambda) + B^s_{jlm} \cdot \sin(m \cdot \lambda) \right] \cdot P_{lm}(\sin \mu) \end{cases}, \quad (19)$$

where $P_{lm}$ are the associated Legendre's polynomials, $\mu$ is the modip latitude (see Eq. 5) and $L$ is the maximum degree of the expansion. For mapping the daily variation of $N_m$F2 and $h_m$F2, we kept the Fourier series expansions with maximum order $J$ given by Eq. (2).

The ITU-R method to compute monthly median values of $f_0$F2 uses two sets of coefficients $(U_{1,0}, \ldots, U_{2J,K})$, one for low and the other for high solar activity. The proposed approach requires one set of $(J+1) \cdot (L+1)^2$ coefficients $(A^c_{0,0,0}, \ldots, A^s_{J,L,L}, B^c_{0,0,0}, \ldots, B^s_{J,L,L})$ (Eqs. (2), (19)) for computing monthly mean values of $N_m$F2 for the solar activity level corresponding to the adjusted period. The same applies to the computation of $h_m$F2.

Summarizing the procedure, the $N_m$F2 and $h_m$F2 (and their standard deviations) estimated in the first step (see Sect. 3.1) are adjusted on a monthly basis by a weighted least squares technique to the functions determined by Eqs. (2) and (19), then obtaining a new set of coefficients the map the F2 peak parameters.

## 4 Results and discussions

### 4.1 The used dataset

The database used in this research is composed of electron density determinations provided by the Constellation Observing System for Meteorology/Formosa Satellite 3 mission (COSMIC/FORMOSAT-3) (Anthes 2008). This mission is a collaborative project between the National Space Organization (NSPO) of Taiwan and the University Corporation for Atmospheric Research (UCAR) of the USA and consists in a constellation of six microsatellites that were launched on April 2006 at an altitude of 512 km of altitude with an inclination of 72° (Cheng et al. 2006). During the first 17 months after the launch the satellites were gradually moved into their final orbits at ~800 km, with a separation of 30° in longitude between the nodes of neighboring orbital planes. The primary payloads of the satellites are GPS radio-occultation receivers, which allow computing profiles of atmospheric refractivity (Kuo et al. 2004). These profiles can be used later to estimate temperature profiles in the stratosphere, temperature and water vapor profiles in the troposphere and electron density profiles (RO profiles) in the ionosphere (Yunck et al. 2000).

The database used in this work was downloaded from the Data Analysis and Archival Center (CDAAC) site (http://cdaac-www.cosmic.ucar.edu/cdaac/products.html), at the UCAR. It includes RO profiles from one continuous month for each solstice and equinox for 2007 (low solar activity) and 2011 (moderate to high solar activity). Between $24 \times 10^3$ and $64 \times 10^3$ profiles, comprising $9.4 \times 10^6$ to $20.8 \times 10^6$ single electron density values were effectively processed for each season. This database provides a very good coverage either in local or in universal time, latitude, longitude and height—from the lower limit of the ionosphere up to the altitude of the satellites (~800 km).

### 4.2 Results

Table 1 contains the number of profiles, N_PR, and single electron density determinations, N_ED, available (AVAIL column) in the CDAAC site and the number that remained after the quality filter step and were processed (PROC) to obtain the final results. Approximately 20 % of the measurements (including $35 \times 10^3$ complete profiles) received negligible weights and for this were eliminated. We have

**Table 1** General description of the used dataset

| Year | Solar activity | Season (day of year) | R12 | N_PR | | N_ED | |
|---|---|---|---|---|---|---|---|
| | | | | AVAIL. | PROC. | AVAIL. | PROC. |
| 2007 | Low | Eq. (080–110) | 11.5 | $70 \times 10^3$ | $64 \times 10^3$ | $26.5 \times 10^6$ | $20.8 \times 10^6$ |
| | | Sol. (180–210) | 13.5 | $55 \times 10^3$ | $51 \times 10^3$ | $22.5 \times 10^6$ | $18.2 \times 10^6$ |
| | | Eq. (250–280) | 4.5 | $45 \times 10^3$ | $42 \times 10^3$ | $19.6 \times 10^6$ | $16.0 \times 10^6$ |
| | | Sol. (330–360) | 8.0 | $58 \times 10^3$ | $54 \times 10^3$ | $25.7 \times 10^6$ | $20.8 \times 10^6$ |
| 2011 | High | Eq. (080–110) | 65.6 | $30 \times 10^3$ | $28 \times 10^3$ | $13.7 \times 10^6$ | $10.8 \times 10^6$ |
| | | Sol. (180–210) | 41.9 | $32 \times 10^3$ | $30 \times 10^3$ | $14.6 \times 10^6$ | $12.0 \times 10^6$ |
| | | Eq. (250–280) | 87.8 | $27 \times 10^3$ | $25 \times 10^3$ | $12.1 \times 10^6$ | $9.5 \times 10^6$ |
| | | Sol. (330–360) | 95.3 | $28 \times 10^3$ | $24 \times 10^3$ | $12.5 \times 10^6$ | $9.4 \times 10^6$ |

'R12' is the 12-month running mean value of the monthly mean sunspot number, 'N_PR' and 'N_ED' are the amount of profiles and electron density values for each case; 'AVAIL.' refers to the available data in the CDAAC database, and 'PROC.' refers to the data that were effectively analyzed

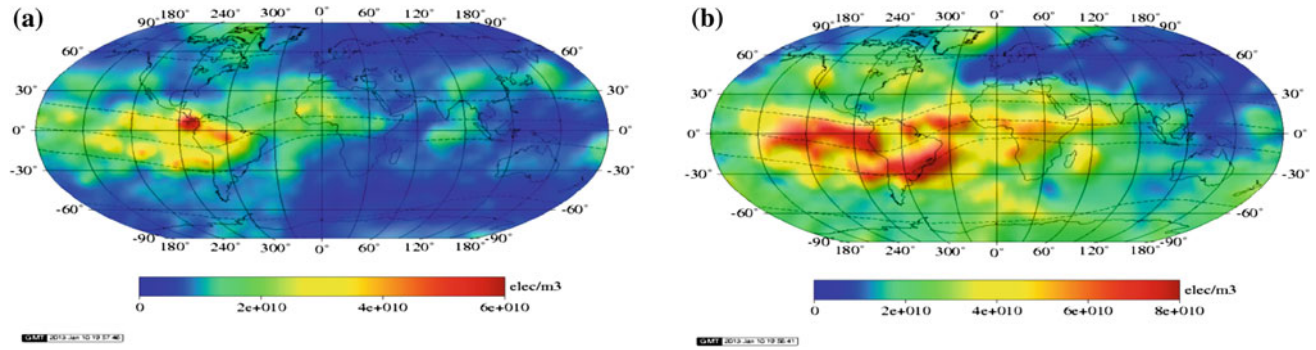


**Fig. 1** Global representation of the RMS difference between the observed and a posteriori computed electron density for the profiles within the 18–20 UT interval of **a** the September equinox of the year 2007; and **b** the December solstice of the year 2011

devoted considerable effort to understand the reasons why these data were discarded. About half of the cases coincided with data, and even complete profiles, that indisputably appeared unrealistic. For the second half, it was difficult to ascertain whether the misalignment between data and models should be attributed to data, the model or both. Nevertheless we have verified that the discarded determinations did not exert significant influence on the final results.

The first step of our analysis consisted in the evaluation of the quality of the adjustment described in Sect. 3.1, i.e. the agreement between the LPIM fitted profiles and the RO electron density determinations. Figure 1a shows a map with RMS of the adjustments for the 18–20 UT interval, the September equinox of 2007. The interval was selected because during these hours the Ionospheric Equatorial Anomaly passes over the South Atlantic geomagnetic anomaly and represents a challenging scenario for modeling. The 2007 September equinox is the period with the lowest solar activity level analyzed in this work. Figure 1b shows the corresponding results for the December of 2011 (the period of highest solar activity analyzed in this work). On average, the RMS of the differences presented in these maps are at about 3 % of the corresponding $N_m$F2 values. Similar statistics were obtained for the other equinoxes and solstices of 2007 and 2011.

The next step in our analysis was the assessment of the propagated errors of the estimated $N_m$F2 parameters. Figure 2a shows the $N_m$F2 estimations obtained with our technique for the 18–20 UT interval least squares adjusting data from 31 days around the September equinox, 2007. Figure 2b shows the corresponding formal errors (standard deviation) obtained in the adjustment. Figure 2c, d shows equivalent maps for the December solstice, 2011. Figure 3 shows the corresponding figures for $h_m$F2. The mean errors computed from these maps are lower than 1 % of the estimated values of the parameters. Similar values were obtained for the other UT intervals and the other equinoxes and solstices of 2007 and 2011.

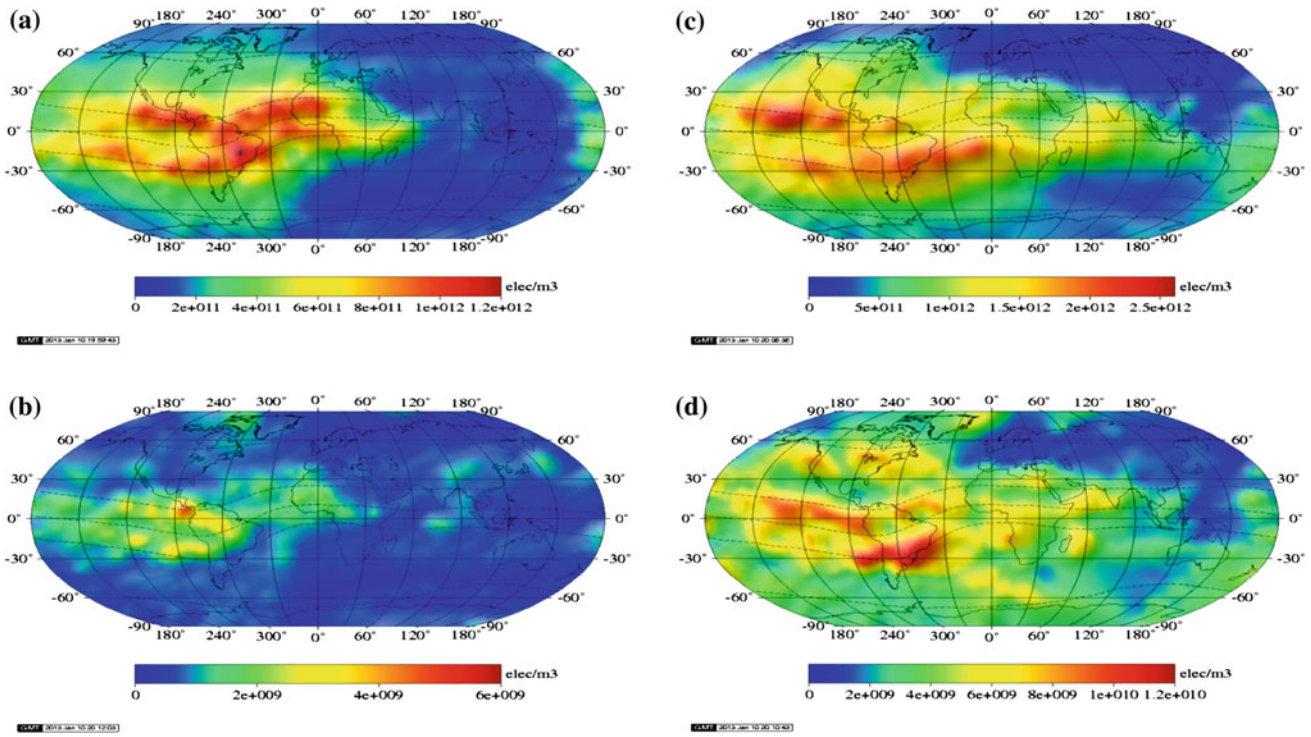


**Fig. 2** Global representation of the $N_m$F2 estimated value and error for the profiles within the 18–20 UT interval: **a** $N_m$F2 for the 2007 September equinox; **b** $N_m$F2 error for the same period; **c** $N_m$F2 for the 2011 December solstice; and **d** $N_m$F2 error for the same period

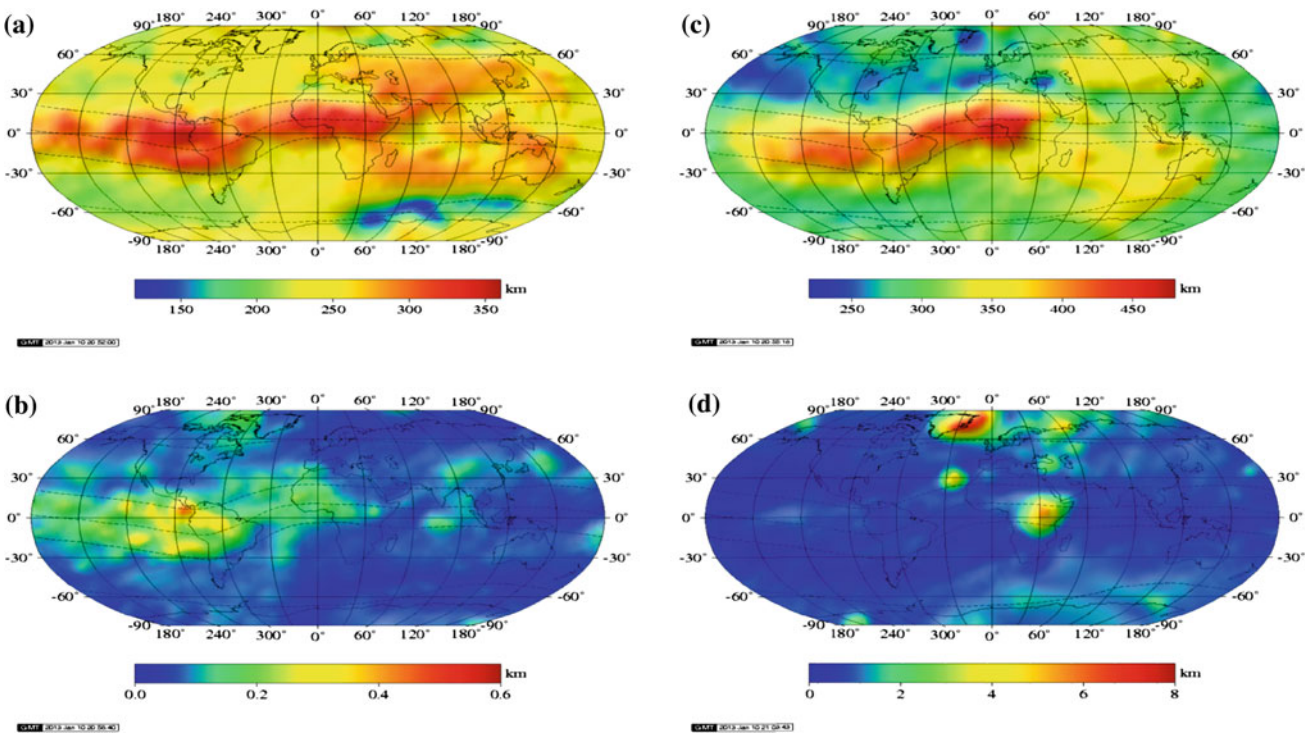


**Fig. 3** Global representation of the $h_m$F2 estimated value and error for the profiles within the 18–20 UT interval: **a** $h_m$F2 for the 2007 September equinox; **b** $h_m$F2 error for the same period; **c** $h_m$F2 for the 2011 December equinox; and **d** $h_m$F2 error for the same period

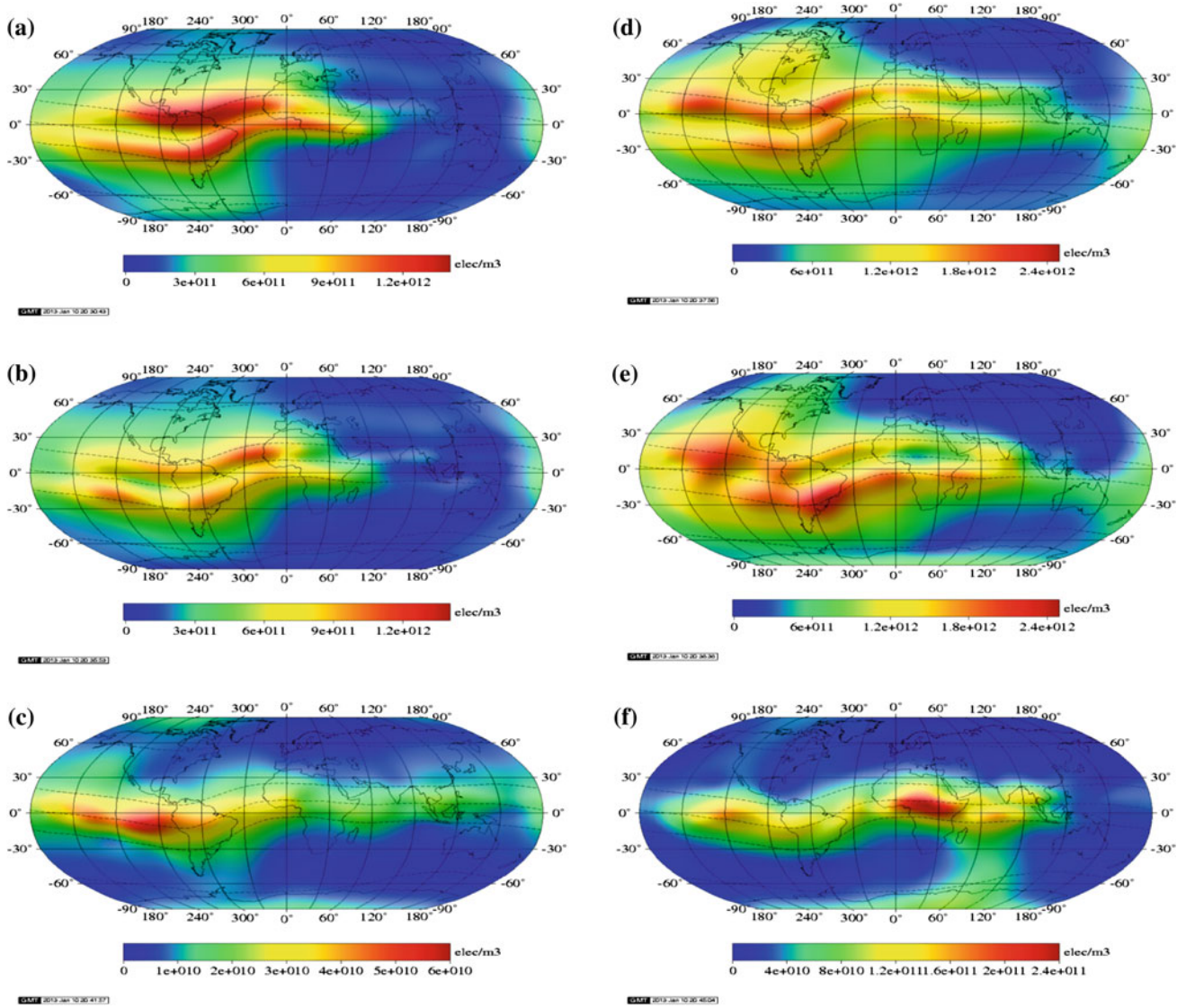


**Fig. 4** Global map of **a** monthly median values of $N_m$F2 computed with the Jones and Gallet technique, at 19 UT, for the September equinox of the year 2007; **b** monthly mean values of $N_m$F2 derived with our technique from the profiles between the 18–20 UT of the September equinox of the year 2007; **c** error of our map; **d** monthly median value of $N_m$F2 computed with the Jones and Gallet technique, at 19 UT, for the December solstice of the year 2011; **e** monthly mean value of $N_m$F2 derived with our technique from the profiles for the 18–20 UT interval of the December solstice; **f** error of our map

Before proceeding to compute the coefficients of the spherical harmonics expansion given by the Eq. (19) we needed to fix the values for $J$ and $L$ (the maximum degrees of the expansion) in order to get the best possible results from the available dataset. For this reason, we applied an analysis of the variance (ANOVA) technique (Weisberg 1980) to evaluate the statistical significance of the terms added to the expansion series, when $J$ and $L$ were increased. For the expansion of $N_m$F2 the ANOVA led us to set $J = 12$ and $L = 9$, implying the estimation of $(J + 1)\cdot(L + 1)^2 = 1200$ coefficients (around 20 % more coefficients than the 988 determined by Jones and Gallet (1962)). For the expansion of $h_m$F2, the ANOVA tests gave $J = 6$ and $L = 8$, implying the estimation of 567 coefficients (around 30 % more than the 441 determined by Jones and Gallet 1962). These maximum degrees permits a temporal/spatial resolution of approximately 1 $^h$/20° for $N_m$F2 and 3 $^h$/22° for $h_m$F2.

Considering the different periods analyzed in this work, the unit-weights standard deviation (Fan 2010), resulting from the Lest Squares adjustments, ranged from $\pm 0.5 \times 10^{10}$ to $\pm 1.2 \times 10^{10}$ elec/m$^{-3}$ for $N_m$F2, and from $\pm 1.7$ to $\pm 3.4$ km for $h_m$F2. The $\chi^2$ statistical test applied to the obtained unit-weight standard deviations did not reject the working hypothesis within a level of significance of 97.5 %.

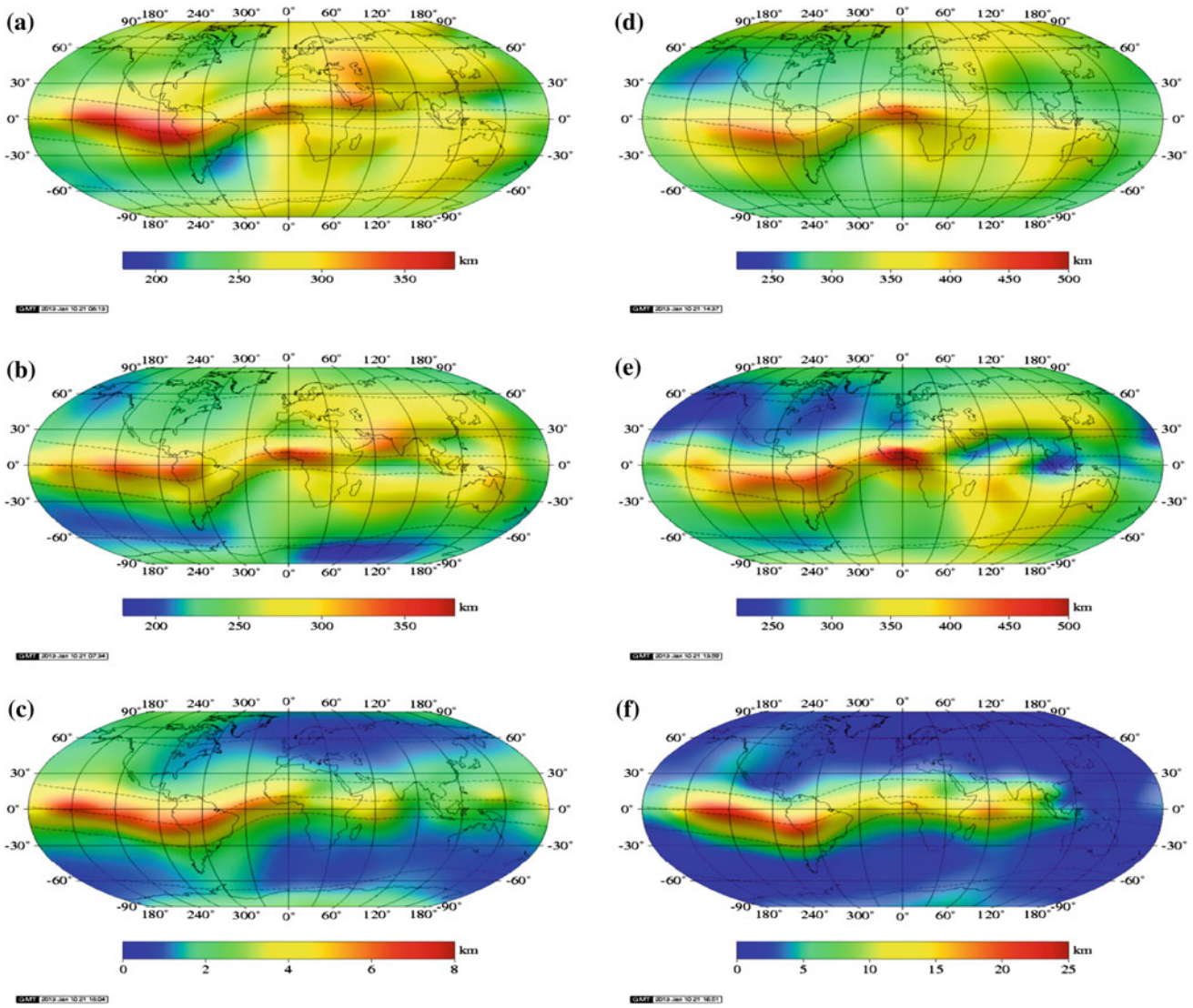


**Fig. 5** Global map of: **a** monthly median values of $h_m$F2 computed with the Jones and Gallet technique, at 19 UT, for the September equinox of the year 2007; **b** monthly mean value of $h_m$F2 derived with our technique form the profiles within the 18–20 UT interval of the September equinox of the year 2007; **c** error of our map; **d** monthly median values of $h_m$F2 computed with the Jones and Gallet technique, at 19 UT, for the December solstice of the year 2011; **e** monthly mean value of $h_m$F2 derived with our technique form the profiles within the 18–20 UT interval of the December solstice of the year 2011; **f** error of our map

### 4.3 Discussion

Figure 4a shows a global map of $N_m$F2 monthly median values computed with the Jones and Gallet (1962) technique for 19 UT, September equinox of 2007. Figure 4b shows the corresponding map computed with our technique and Fig. 4c shows the map for the estimated errors. Figure 4d–f shows the equivalent maps for December solstice of 2011. Figure 5 shows the equivalent results for $h_m$F2.

The analysis of Figs. 4 and 5 (and other similar figures representative of the other time intervals, seasons and years considered in this work) shows that the largest errors in the estimation of both $N_m$F2 and $h_m$F2 are found in the region of the Equatorial Anomaly. This effect is a direct consequence of the difficulty to model the electron density distribution in that region and, up to some extent, to the limitations of the RO technique in regions of steep horizontal gradients. The geographic behavior of the errors is also modulated by the data coverage. For example, a clear amplification of the errors over the modip equator in the African continent is produced by the scarcity of RO profiles in that region.

The global mean errors ranged from $0.5 \times 10^{10}$ to $3.6 \times 10^{10}$ elec/m$^{-3}$ for $N_m$F2 (approximately 7 % of the value of the estimated parameter) and from 2.0 to 5.6 km for $h_m$F2 ($\sim$2 %).

For $N_m$F2, the largest differences between the Jones and Gallet (1962) and our maps are observed over the Central/South American, Atlantic and African sectors, in a band approximately within ±45° of modip latitude, when the Equatorial Anomaly is developed over those sectors. The differences range from approximately $\pm 80 \times 10^{10}$ elec/m$^{-3}$ for high solar activity to approximately $+20 \times 10^{10}/-50 \times 10^{10}$ elec/m$^{-3}$ for low solar activity. For $h_m$F2, the largest differences are around ±80 km for both, high and low solar activity conditions. These largest differences appear in different parts of the globe, depending on the time interval, season and year, but a positive difference (our $h_m$F2 values are larger than the Jones and Gallet values 1962) tends to occur over the Equatorial Anomaly close to the solar terminator sector.

### 4.4 Summary and conclusion

This work presents a technique that we have developed to routinely update the ITU-R F2 peak dataset, using RO electron density profiles derived from GPS receivers flying on low Earth orbiter satellites. The technique is used to compute two sets of coefficients for computing monthly mean values of $N_m$F2 and $h_m$F2, for any given latitude, longitude and UT, and for the current solar activity level. Along with the development we have slightly modified the mathematical formulation recommended by the ITU-R so that IRI and NeQuick models could implement our dataset without the need of significant changes on the source codes.

A critical point of our work was the quality evaluation of the RO profiles (i.e. the acceptance of a profile as a valid one) that are the primary input of our technique. After quality filtering the input data, every RO profile available for the analyzed period was fitted to the LPIM profile using a Least Squares adjustment and an iteratively re-weighting scheme. The previous step provided $N_m$F2 and $h_m$F2 values accompanied with estimations of their errors (standard deviations) for every RO profile. These set of values were used to compute, in a monthly basis and with a Least Squares method, two sets of numerical coefficients for the global mapping the $N_m$F2 and $h_m$F2. The geographical variation of the parameters was modeled with a spherical harmonic expansion series and the diurnal variation with Fourier expansion series. The maximum degrees of these expansions were established through an ANOVA test, which led to maximum degrees equal to 12 (geographical variation) and 9 (diurnal variation) for $N_m$F2, and 6 and 8 for $h_m$F2.

We tested our technique using the RO profiles produced by the COSMIC/FormoSat 3 team, for the 4 months (solstices and equinoxes) of one low and one high solar activity year (each month at a time). The RMS of the differences between RO and modeled values did not exceed 3 % of the $N_m$F2 value of the corresponding profiles We have also analyzed error propagation into the estimated parameters and found errors that did not exceed 1 %. The unit-weight standard deviation resulting from the Least Squares adjustments ranged from $\pm 0.5 \times 10^{10}$ to $\pm 1.2 \times 10^{10}$ elec/m$^{-3}$ for $N_m$F2, and from ±1.7 to ±3.4 km for $h_m$F2. A $\chi^2$ test was applied to these values and the result is that we cannot reject the proposed model (spherical harmonic and Fourier expansion series, Sect. 3.2) with a significance level of 97.5 %. Furthermore, the error propagation law was conducted to estimate the errors of the maps, which ranged from $0.5 \times 10^{10}$ to $3.6 \times 10^{10}$ elec/m$^{-3}$ for $N_m$F2 (approximately 7 % of the mapped parameter) and from 2.0 to 5.6 km for $h_m$F2 (approximately 2 % of the mapped parameter).

Regarding the differences of $N_m$F2 and $h_m$F2 between the values computed with the Jones and Gallet (1962) and our technique, we saw that the largest errors for both parameters are found in region of the Equatorial Anomaly. This fact could be related to difficulties to model the electron density distribution in that region and, up to some extent, to the limitations of the RO technique to accurate values in regions of steep horizontal gradients. The largest differences for the $N_m$F2 ranged from approximately $\pm 80 \times 10^{10}$ elec/m$^{-3}$ for high solar activity to $+20 \times 10^{10}/-50 \times 10^{10}$ elec/m$^{-3}$ for low solar activity. The corresponding differences for the $h_m$F2 maps are around ± 80 km for both, high and low solar activity conditions.

**Acknowledgments** The authors thank Dr. R. Klees and Dr. J. Böhm for their constructive comments.

## References

Altinay O, Tulunay E, Tulunay Y (1997) Forecasting of ionospheric critical frequency using neural networks. Geophys Res Lett 24: 1467–1470

Angling MJ (2008) First assimilations of COSMIC radio occultation data into the Electron Density Assimilative Model (EDAM). Ann Geophys 26:353–359. doi:10.5194/angeo-26-353-2008

Anthes RA, Bernhardt PA, Chen Y, Cucurul L, Dymond KF, Ector D, Healy SB, Ho S-P, Hunt DC, Kuo Y-H, Liu H, Manning K, Mccormick C, Meehan TK, Randel WJ, Rocken C, Schreiner WS, Sokolovskiy SV, Syndergaard S, Thompson D, Trenberth KE, Wee T-K, Yen NL, Zeng Z (2008) The COSMIC/FORMOSAT 3 mission–early results. Bull Am Meteorol Soc March 89:313–333

Azpilicueta F, Brunini C (2008) Analysis of the bias between TOPEX and GPS vTEC determinations. J Geod. doi:10.1007/s00190-008-0244-7

Bilitza D (2001) International reference ionosphere 2000. Radiol Sci 36(2):261–275

Bilitza D (2002) Ionospheric models for radio propagation studies. In: Review of radio science 1999–2002. Oxford University Press, NY, pp 625–679

Bilitza D, Brown S, Wang MY, Souza JR, Roddy PA (2012) Measurements and IRI model predictions during the recent solar minimum. J Atmos Solar Terr Phys 86:99–106. doi:10.1016/j.jastp.2012.06.010

Bilitza D, Sheikh M, Eyfrig R (1979) A global model for the height of the F2-peak using M3000 values from the CCIR numerical map. Telecomm J 46(9):549–553

Bradley PA, Dudeney JR (1973) A simple model of the vertical distribution of electron concentration in the ionosphere. J Atmos Solar Terr Phys 35(12):2131–2146

Brunini C, Azpilicueta F, Gende M, Camilion E, Aragón Ángel A, Hernandez-Pajares M, Juan M, Sanz J, Salazar D (2011) Ground- and space-based GPS data ingestion into the NeQuick model. J Geod. doi:10.1007/s00190-011-0452-4

Brunini C, Azpilicueta F, Gende M, Camilion E, Gularte E (2013a) Improving SIRGAS ionospheric model. In: International Association of Geodesy symposia, vol 138, pp 245–250 (in press)

Brunini C, Meza A, Bosch W (2005) Temporal and spatial variability of the bias between TOPEX and GPS derived TEC. J Geod 79:175–188. doi:10.1007/s00190-005-0448-z

Bruninia C, Conte JF, Azpilicueta F, Bilitza D (2013b) A different method to determine the height of the F2 peak. Adv Space Res (in press)

CCIR (1991) Report 340–6. Comité Consultatif International des Radio communications, Genève, Switzerland

Cheng C-Z, Kuo Y-H, Anthes RA, Wu L (2006) Satellite constellation monitors global and space weather. Eos Trans Am Geophys Union 87:166–167

Codrescu MV, Beierle KL, Fuller-Rowell TJ (2001) More total electron content climatology from TOPEX/Poseidon measurements. Radio Sci 36(2):325–333

Delay S, Doherty P (2004) A decade of ionospheric measurements from the TOPEX/Poseidon mission, contribution to the International Beacon Satellite Symposium, Trieste, October 18th-22nd

Dudeney JR (1975) A simple empirical method for estimating the height and semi-thickness of the F2-layer at the Argentine Islands Graham Land. British Antarctic Survey, Science Report No 88, London

Eyfrig R (1973) Eine Bemerkung zur Bradley–Dudeney'schen Modell-Ionosphäre. Kleinheubacher Berichte 17:199–202

Fan H (2010) Theory of errors and least squares adjustment. Royal Institute of Technology, Division of Geodesy and Geoinformatics, 100 44 Stockholm, Sweden. ISBN 91-7170-200-8

Fox MW, McNamara LF (1988) Improved world-wide maps of monthly median of foF2. J Atmos Terr Phys 50:1077–1086

Gulyaeva TL, Bradley PA, Stanislawska I, Juchnikowski G (2008) Towards a new reference model of hmF2 for IRI. Adv Space Res 42:666–672. doi:10.1016/j.asr.2008.02.021

Hernandez-Pajares M (2003) Performance of IGS Ionosphere TEC maps. Presented at 22nd IGS Governing Board Meeting, Nice, 6th April

Hoque MM, Jakowski N (2011) A new global empirical NmF2 model for operational use in radio systems. Radio Sci 46:RS6015. doi:10.1029/2011RS004807

Hoque MM, Jakowski N (2012) A new global model for the ionospheric F2 peak height for radio wave propagation. Ann Geophys. doi:10.5194/angeo-30-797-2012

Huber PJ (1981) Robust Statistics. Wiley, London

ITU-R(1997) Recommendation ITU-R P 1239. ITU-R reference ionospheric characteristics, International Telecommunications Union, Radio Communication Sector, Geneva

Jakowski N, Leitinger R, Angling M (2004) Radio occultation techniques for probing the ionosphere. Ann Geophys 47:1049–1066

Jones WB, Gallet RM (1962) Representation of diurnal and geographical variations of ionospheric data by numerical methods. ITU Telecomm J 29(5):129–149

Jones WB, Gallet RM (1965) Representation of diurnal and geographical variations of ionospheric data by numerical methods, II. Control of Stability. ITU Telecomm J 32(1):18–28

Jones WB, Obitts DL (1970) Global representation of annual and solar cycle variations of foF2 monthly median 1954–1958. Telecommunications Research Report, OT/ITS/RR3, Washington DC, USA, US Government Printing Office

Kuo Y-H, Wee T-K, Sokolovskiy S, Rocken C, Schreiner W, Hunt D, Anthes RA (2004) Inversion and error estimation of GPS radio occultation data. J Meteor Soc Japan 82:507–531

Liu C, Zhang M-L, Wan W, Liu L, Ning B (2008) Modeling M(3000)F2 based on empirical orthogonal function analysis method. Radio Sci 43:RS1003. doi:10.1029/2007RS003694

Meza A, Gularte Scarone E, Brunini C, Mosert M (2008) Analysis of a topside ionospheric model using GPS and ionosonde observables. Adv Space Res 42:712–719. doi:10.1016/j.asr.2007.08.042

Nava B, Coïsson P, Radicella SM (2008) A New version of the NeQuick ionosphere electron density model. J Atmos Sol Terr Phys, pp 1856–1862. doi:10.1016/j.jastp.2008.01.015

Obrou OK, Bilitza D, Adeniyi JO, Radicella SM (2003) Equatorial F2-layer peak height and correlation with vertical ion drift and M(3000)F2. Adv Space Res 31(3):513–520

Oyeyemi EO, Poole AWV, McKinnell LA (2005) On the global model for foF2 using neural networks. Radio Sci 40:RS6011. doi:10.1029/2004RS003223

Rawer K (ed) (1984) Encyclopedia of physics. Geophysics III, Part VII. Springer, Berlin, pp 389–391

Rawer K, Eyfrig R (2004) Improving the M(3000)-$h_M$F2 relation. Adv Space Res 33:878–879

Reinisch BW, Huang X (2001) Deducing topside profiles and total electron content from bottomside ionograms. Adv Space Res 27(1):23–30

Rush C, Fox M, Bilitza D, Davies K, McNamara L, Stewart F, PoKempner M (1989) Ionospheric mapping—an update of foF2 coefficients. Telecomm J 56:179–182

Rush CM, Pokempner M, Anderson DN, Stewart FG, Perry J (1984) Maps of foF2 derived from observations and theoretical data. Radio Sci 19:1083–1097

Schreiner W, Rocken C, Sokolovskiy S, Syndergaard S, Hunt D (2007) Estimates of the precision of GPS radio occultations from the COSMIC/FORMOSAT-3 mission. Geophys Res Lett 34:L04808. doi:10.1029/2006GL027557

Shimazaki T (1955) World-wide daily variation in the height of the maximum electron density of the ionospheric F2-layer. J Radiol Res Lab 2(7):85–97

Weisberg S (1980) Applied linear regression. Wiley, New York

Wintoft P, Cander LJR (1999) Short-term prediction of foF2 using time delay neural networks. Phys Chem Earth(c) 24:343–347

Wright JW, Mcduffie RE (1960) The relation of $h_M$F2 to M(3000)F2 and $h_p$F2. J Radio Res Lab (Tokyo) 7(32):498–520

Yue X, Schreiner WS, Lei J, Sokolovskiy SV, Rocken C, Hunt DC, Kuo Y-H (2010) Error analysis of Abel retrieved electron density profiles from radio occultation measurements. Ann Geophys 28:217–222. doi:10.5194/angeo-28-217-2010

Yunck TP, Liu C-H, Ware R (2000) A history of GPS sounding. Terr Atmos Oceanic Sci 11:1–20

Zhang M-L, Liu C, Wan W, Liu L, Ning B (2009) A global model of the ionospheric F2 peak height based on EOF analysis. Ann Geophys 27:3203–3212. doi:10.5194/angeo-27-3203-2009